

Decomposition of Nonlinear Dynamical Systems Using Koopman Gramians

Zhiyuan Liu, Soumya Kundu, Lijun Chen, and Enoch Yeung

Abstract—In this paper we propose a new Koopman operator approach to the decomposition of nonlinear dynamical systems using Koopman Gramians. We introduce the notion of an input-Koopman operator, and show how input-Koopman operators can be used to cast a nonlinear system into the classical state-space form, and identify conditions under which input and state observable functions are well separated. We then extend an existing method of dynamic mode decomposition for learning Koopman operators from data known as deep dynamic mode decomposition to systems with controls or disturbances. We illustrate the accuracy of the method in learning an input-state separable Koopman operator for an example system, even when the underlying system exhibits mixed state-input terms. We next introduce a nonlinear decomposition algorithm, based on Koopman Gramians, that maximizes internal subsystem observability and disturbance rejection from unwanted noise from other subsystems. We derive a relaxation based on Koopman Gramians and multi-way partitioning for the resulting NP-hard decomposition problem. We lastly illustrate the proposed algorithm with the swing dynamics for an IEEE 39-bus system.

I. INTRODUCTION

The design and control of complex systems is usually broken down into simpler modules, e.g. different geographically dispersed subsystems such as different balancing authority areas in power networks and various vertically integrated functionalities such as routing and congestion control in communication networks. Despite modular design being a common practice, the decomposition of the system into different modules is often based on engineering intuition rather than principled methodologies.

For example, in some applications, the physical layout or construction of a system dictates the subsystem structure. For example, in multi-cellular biological systems, the subsystems are a natural consequence of physical separation by the membrane barrier [1], [3], [2]. In critical infrastructure systems, e.g. the power grid or water distribution systems, the subsystem structure is traditionally defined based on distance and connectivity of buses, nodes or junctions [4], [5]. However, this choice of decomposition is critical since a poor system or model decomposition can introduce fundamental limits into distributed controller performance.

Moreover, there are many scenarios where a suitable system decomposition may not be known *a priori*, e.g. design of large-scale or ad-hoc communication networks [8],

Z. Liu and L. Chen are with the Department of Computer Science, University of Colorado, Boulder, CO 80309, USA (email: {zhiyuan.liu, lijun.chen}@colorado.edu),

S. Kundu and E. Yeung are with the Pacific Northwest National Laboratory, Richland, WA 99354, (email: {soumya.kundu, enoch.yeung}@pnl.gov).

[9], [4] or cyber-physical systems made of agile teams of agents. In such situations, the system decomposition must be identified, using appropriate criteria that enable performance of a distributed controller. This is especially true of extremely large scale networks involving thousands of variables where synthesis of a global controller may not be computationally feasible.

There are many existing methods for model decomposition [10], [11], [9]; each method decomposes systems based on different properties. Sanchez-Garcia et al. [10] decomposes a system into subsystems by examining the spectrum of a matrix encoding connectivity in power networks. When that matrix is the admittance matrix, the decomposition reflects static connectivity structure; when the matrix is power flow, the decomposition reveals islands with minimal power flow disruption. Chiang, Low, and Doyle showed that system decomposition for layered network design problems can be thought of as vertical and horizontal decomposition of optimization problems with utility functions corresponding to different Quality of Service metrics, e.g. fairness, minimal congestion, or efficiency [9]. Raak et al. [11] use the Koopman operator to define a lifted linear representation of an open-loop nonlinear system. They introduce a decomposition method based on the point-spectrum of the Koopman operator.

In this paper we adopt a similar Koopman operator approach for system decomposition as Raak et al. [11], but derive the decomposition from input-output properties directly computed from Koopman Gramians [12]. Koopman operators are especially powerful, since they allow us to transform nonlinear analysis and control problems into linear problems. Furthermore, system identification methods for Koopman operators have made it possible to perform analysis and control design in a purely data-driven fashion [13], [14], [15], [16]. Such an approach is especially valuable in data-driven control and analysis problems, e.g., Internet of Things applications [8], intelligent load control problems in infrastructure systems [17], or design of multicellular biocircuits [3].

Specifically, we introduce the notion of an input-Koopman operator, show how input-Koopman operators can be used to cast a nonlinear system into the classical state-space form, and identify conditions under which input and state observable functions are well separated. We then extend an existing method of dynamic mode decomposition for learning Koopman operators from data known as deep dynamic mode decomposition to systems with controls or disturbances. We illustrate the accuracy of the method in

learning an input-state separable Koopman operator for an example system, even when the underlying system exhibits mixed state-input terms. We next introduce a nonlinear decomposition algorithm, based on Koopman Gramians, that maximizes internal subsystem observability and disturbance rejection from unwanted noise from other subsystems. As the resulting decomposition problem is NP-hard, we derive a relaxation based on Koopman Gramians and multi-way partitioning. We illustrate the proposed algorithm with the swing dynamics for an IEEE 39-bus system

The rest of the paper is organized as follows. Section II introduces input-Koopman operators and reviews the theory of input-Koopman operators. Section III discusses several results and techniques for learning Koopman operators and the associated Koopman Gramians. Section IV presents the proposed Koopman decomposition algorithm, and Section V illustrates its application on an IEEE 39-bus system.

II. INPUT-KOOPMAN OPERATORS

In [18], [19], it was shown that the Koopman operator could be generalized to model the effect of inputs or controls. The authors showed that an input-Koopman operator K could be defined that satisfies

$$\begin{aligned}\psi(x_{t+1}, w_{t+1}) &= K \circ \psi(x_t, w_t) \\ &= \psi(f(x_t, w_t)).\end{aligned}\quad (1)$$

where $\psi(x_t, w_t) \in \mathbb{R}_L^n$, $n_L \leq \infty$ is a potentially infinite-dimensional dictionary of observables defined on the state x_t and the input w_t . Thus, K is a linear operator with a well-defined spectrum, either discrete and countable, or continuous and uncountably infinite. In this paper, we consider the scenario where K is a finite or countably infinite dimensional operator.

Assumption 1: We suppose that the system (14) has a finite or countably infinite dimensional Koopman operator. If the control inputs have their own dynamics, e.g. they are defined by the state-space dynamics of a controller, then $\psi(x_{t+1}, w_{t+1})$ defines a linear state-space model for x_t and w_t . In the case where w_t has no state-dynamics, e.g. it is modeled as an exogenous input or random disturbance, then the input-Koopman operator K satisfies

$$\psi(x_{t+1}, 0) = K\psi(x_t, w_t) \quad (2)$$

For the purposes of this paper, both for defining Koopman gramians and performing input-Koopman analysis, we model inputs as disturbances without state-space dynamics.

Assumption 2: Given the Koopman model (1) for the nonlinear time-invariant system (14)

$$\psi(x_{t+1}, w_{t+1}) = \psi(x_{t+1}, 0) = K\psi(x_t, w_t) \quad (3)$$

In essence, we model inputs as purely exogenous, impulse functions, or random disturbances to the system of interest. This assumption is equivalent to saying that w_t is not necessary to include into $\psi(\cdot)$ in order to satisfy the axiom of state for the dynamical system (5). The consequence of this assumption is that we can express the system in affine Koopman control form.

Lemma 1: Consider a nonlinear system of the form

$$x_{t+1} = f(x_t, w_t) \quad (4)$$

with exogenous disturbances w_t and corresponding Koopman model satisfying Assumption 2,

$$\psi(x_{t+1}, 0) = K\psi(x_t, w_t). \quad (5)$$

The same Koopman equation can be written as

$$\psi_x(x_{t+1}) = K_x\psi_x(x_t) + K_u\psi_u(u_t) \quad (6)$$

where $u_t = u(x_t, w_t)$ is a vector function consisting of univariate terms of w_t and multivariate polynomial terms consisting of x_t and w_t .

Proof: Consider the nonlinear system (4). We remark the form of equation (5) is a special instance of the form derived in [18]. To be precise, the existence of a closed-loop system Koopman operator that satisfies the relation

$$\psi(x_{t+1}, w_{t+1}) = K\psi(x_t, w_t) \quad (7)$$

follows from the original Koopman papers [20], [21]. The entire state-space dynamics of a closed-loop nonlinear system, including both state and input, can be viewed as the state-space dynamics of an autonomous dynamical system which has a Koopman operator. Moreover, Assumption 2 guarantees that the system can be written in the form

$$\psi_x(x_{t+1}) = K\psi(x_t, w_t) \quad (8)$$

where $\psi_x(\cdot)$ is a vector consisting of the elements of $\psi(x_t, w_t)$ that only depend on x_t . Due to Assumption 1 we know that K is a linear operator that can be represented by a matrix of countable dimension. Therefore, the right hand side can be partitioned in terms of dependence of Koopman basis functions on x_t, w_t or both x_t and w_t :

$$\psi_x(x_{t+1}) = K_x\psi_x(x_t) + K_{xw}\psi_{xw}(x_t, w_t) + K_w\psi_w(w_t) \quad (9)$$

where $\psi_x(x_t)$ represents the elements of $\psi(x_t, w_t)$ that directly depend on x_t , $\psi_{xw}(x_t, w_t)$ represents the elements of $\psi(x_t, w_t)$ that depend on a mixture of x_t and w_t terms, and $\psi_w(w_t)$ represents the elements of $\psi(x_t, w_t)$ that only depends on w_t . Now consider the last two terms on the right hand side; we can write an exact expression according to Taylor's theorem for each term

$$\psi_{xw}(x_t, w_t) = W_{xw}\nu(x_t, w_t) \quad (10)$$

where $\nu(x_t, w_t)$ is a vector containing the polynomial basis with elements of the form

$$x_i^l w_j^k, \quad (11)$$

$l, k \in \mathbb{N}$, x_i is an element of the state vector x , $i = 1, 2, \dots$ and w_j is an element of the disturbance vector w , $j = 1, 2, \dots$ Similarly, $\nu(w_t)$ is a vector containing the polynomial basis with elements of the form

$$w_i^l w_j^k \quad (12)$$

where $i, j = 1, 2, \dots$ and $l, k \in \mathbb{N}$. Define

$$u_t = [w_t^T \quad \nu(x_t, w_t)^T]^T$$

It immediately follows that

$$K_u = \begin{bmatrix} K_w \\ K_{xw} W_{xw} \end{bmatrix}$$

and therefore

$$\psi_x(x_{t+1}) = K_x \psi_x(x_t) + K_u \psi_u(u_t) \quad (13)$$

Finally, we suppose that the observable functions retain the information of the underlying output y_t , via a projection.

Assumption 3: We suppose, as in [16], that there exists a $W_h \in \mathbb{R}^{p \times n_L}$ such that

$$y_t = h(P_x \psi_x(x_t)) = W_h \psi_x(x_t)$$

is in the span of the observables $\psi_x^1(x_t), \dots, \psi_x^N(x_t)$.

This assumption is important for the formulation of a Koopman observability gramian [12].

We now consider a class of nonlinear systems which have state-control separability. Specifically, we consider systems like (4) with the explicit form

$$\begin{aligned} x_{t+1} &= f(x_t) + g(w_t) \\ y_t &= h(x_t) \end{aligned} \quad (14)$$

where $f, g, h \in \mathbb{R}^n$ is assumed to be continuously differentiable functions (with $f, g \in C^p[0, \infty)$ where $p \geq 2$) with respect to x and w , respectively. Without loss of generality, we suppose that $w_t = 0$ implies that $g(w) = 0$, i.e. any zeroth-order terms in a Taylor expansion of $g(w)$ are subsumed into the definition of $f(x)$ as an affine constant offset.

Lemma 2: Consider a state-input separable system of the form (14). Suppose the system satisfies Assumptions 1 and 2. Let K_x denote a Koopman operator for the corresponding open loop system

$$\begin{aligned} x_{t+1} &= f(x_t) \\ y_t &= h(x_t) \end{aligned} \quad (15)$$

such that

$$\psi_x(x_{t+1}) = \psi_x(f(x)) = K_x \circ \psi_x(x_t) \quad (16)$$

If there exists functions ψ_{xw}, ψ_w and matrices K_{xw}, K_w such that

$$\begin{aligned} \psi_x(x_{t+1}(x_t, w_t)) - \psi_x(x_{t+1}(x_t, 0)) &= K_{xw} \psi_{xw}(x_t, w_t) \\ &\quad + K_w \psi_w(x_t, w_t) \end{aligned} \quad (17)$$

then

$$\begin{bmatrix} \psi_x(x_{t+1}) \\ \psi_{xw}(x_{t+1}, w_{t+1}) \\ \psi_w(w_{t+1}) \end{bmatrix} = \begin{bmatrix} K_x & K_{xw} & K_w \end{bmatrix} \begin{bmatrix} \psi_x(x_t) \\ \psi_{xw}(x_t, w_t) \\ \psi_w(w_t) \end{bmatrix} \quad (18)$$

and

$$K = \begin{bmatrix} K_x & K_{xw} & K_w \end{bmatrix} \quad (19)$$

is a Koopman operator for the w_t -perturbed system (14). Finally, if i) $\psi_{xw}(x, w)$ defines a basis set on x even when $w = 0$ and ii) $\psi_x(x)$ is continuous, then

$$K_{xw} \equiv 0.$$

Proof: Suppose that there exists functions ψ_{xw}, ψ_w and matrices K_{xw}, K_w such that

$$\begin{aligned} \psi_x(x_{t+1}(x_t, w_t)) - \psi_x(x_{t+1}(x_t, 0)) &= K_{xw} \psi_{xw}(x_t, w_t) \\ &\quad + K_w \psi_w(x_t, w_t) \end{aligned} \quad (20)$$

Since K_x is the open-loop Koopman operator,

$$\begin{aligned} \psi_x(x_{t+1}(x_t, 0)) &= \psi_x(f(x) + g(0)) \\ &= \psi_x(f(x)) \\ &= K_x \psi_x(x_t) \end{aligned} \quad (21)$$

which proves equation (18). Next, suppose that K_w has full column rank and $\psi_x(x)$ is continuous. Then taking the limit as $w_t \rightarrow 0$ to obtain

$$\lim_{w_t \rightarrow 0} \psi_x(x_{t+1}(x_t, w_t)) - \psi_x(x_{t+1}(x_t, 0)) = 0 \quad (22)$$

which implies that

$$0 = \lim_{w_t \rightarrow 0} K_{xw} \psi_{xw}(x_t, w_t) + K_w \psi_w(w_t). \quad (23)$$

Now $-K_w \psi_w(0)$ is a constant vector, if it is a non-zero constant vector then we would obtain a contradiction since $\psi_{xw}(x, 0)$ is a function in x . Thus, $-K_w \psi_w(0) = 0$, which implies that

$$K_{xw} \psi_{xw}(x_t, 0) = -K_w \psi_w(0) = 0 \quad (24)$$

and since $\psi_{xw}(x_t, 0)$ is a basis with respect to x_t , this means that the matrix

$$[\psi_{xw}(x_1, 0) \quad | \quad \dots \quad | \quad \psi_{xw}(x_S, 0)] \quad (25)$$

is right invertible as long as $S \geq \dim(\psi_{xw})$, which implies that $K_{xw} \equiv 0$. ■

III. DEEP DYNAMIC MODE DECOMPOSITION FOR CONTROL-KOOPMAN OPERATOR LEARNING

The traditional method for learning a Koopman operator from data is extended dynamic mode decomposition. In extended dynamic mode decomposition for open-loop systems, a dictionary of empirical observable functions

$$\Psi(x) = \{\psi_1(x), \psi_2(x), \dots, \psi_{n_D}(x)\} \quad (26)$$

is postulated to span a large enough subspace of the true Koopman (and unknown observable functions).

In input-Koopman (or control-Koopman) learning problems [18], [19] for systems satisfying Assumption 2, a dictionary of empirical observable functions is defined in terms of the system state $x \in \mathbb{R}^n$ and input $w \in \mathbb{R}^m$ of the form

$$\Psi(x, u) = \{\psi_x(x), \psi_{xw}(x, w), \psi_w(w)\} \quad (27)$$

where $\psi_x(x) \in \mathbb{R}^{n_L}$ and $(\psi_{xw}(x, w), \psi_w(w)) \in \mathbb{R}^{m_L}$. Again, the challenge is that the true Koopman state and input observable functions are unknown.

In general, there always exists a trivial Koopman observable function $\psi_x(x) \equiv 0$ and $(\psi_{xw}(x, w), \psi_w(w)) \equiv 0$ with corresponding trivial control and state Koopman matrices $K_x \equiv 0$ and $K_w \equiv 0$. Such Koopman representations are not of interest to us, since ultimately we are interested finding concise representations that elucidate underlying system dynamics, in terms of the state x_t and w_t . Thus, we adopt the classical assumption of including the state x_t and disturbance w_t in the dictionary functions.

Assumption 4: Let $\Psi(x, u)$ denote the Koopman observable dictionary. We suppose that there exists a collection of $\psi_{x,1}(x), \dots, \psi_{x,n}(x), \psi_{w,1}(w), \dots, \psi_{w,m} \in \Psi(x, u)$ such that

$$(\psi_{x,1}(x_t), \dots, \psi_{x,n}(x_t)) = x_t \in \mathbb{R}^n \quad (28)$$

and

$$(\psi_{w,1}(w_t), \dots, \psi_{w,m}(w_t)) = w_t \in \mathbb{R}^m \quad (29)$$

We refer to such a dictionary $\Psi(x, u)$ satisfying these properties as *state and input inclusive*.

Given a system (4), with time series data y_1, \dots, y_t the control-Koopman learning problem is to find a set of observable functions $\psi_x(x), \psi_w(w)$, and $\psi_{xw}(x, w)$, and matrices $K_x \in \mathbb{R}^{n_L \times n_L}, W_h \in \mathbb{R}^{p \times n_L}$ and $[K_{xw} \ K_w] \in \mathbb{R}^{n_L \times m_L}$ to solve the optimization problem

$$\min_{W_h, \psi_x, \psi_w, \psi_{xw}, K_{xw}, K_w, K_x} \|Y_{t:1} - F_{t-1:0}\| \quad (30)$$

where

$$Y_{t:1} = [y_t \ y_{t-1} \ \dots \ y_1] \quad (31)$$

and

$$F_{t-1:0} = [\kappa(t-1) \ \dots \ \kappa(1),] \quad (32)$$

with

$$\begin{aligned} \kappa(t-1) = & -W_h(K_x \psi_x(x_{t-1}) + K_{xw} \psi_{xw}(x_{t-1}, w_{t-1}) \\ & + K_w \psi_w(w_{t-1})). \end{aligned} \quad (33)$$

In general, learning the Koopman observable functions for both the input and state can be computationally expensive. Typically, a generic but expressive set of dictionary functions such as Hermite polynomials, Legendre polynomials or thin-plate radial basis functions are used [16]. However, the number of dictionary functions required is not known a priori and often the number of dictionary terms requires multiple steps of manual refinement, even for the simple two or three state systems.

Recently, it was shown that deep (and shallow) neural networks can be used to generate Koopman observable dictionaries that automatically update during the training process [22], [23]. Moreover, the dictionaries learned using neural networks appear to be efficient at encoding Koopman dictionaries for larger systems, e.g. a partially observed large-scale linear system and a glycolytic oscillator with 7 states.

We extend the methods developed in [22], to address the input-Koopman operator learning problem. In particular, we suppose that ψ_x, ψ_{xw} , and ψ_w are the outputs of three separate neural networks that multiply against decision variables $K_x, K_{x,w}$ and K_w respectively. The learning objective is thus

defined as the Frobenius norm of objective function (30). In particular, the deep neural networks allow us to parameterize the Koopman observable functions as follows:

$$\begin{aligned} \psi_x(x) &= (x, \mathcal{D}_x(x, \theta_x)) \\ \psi_w(w) &= (w, \mathcal{D}_w(w, \theta_w)) \\ \psi_{xw}(x, w) &\approx \mathcal{D}_{xw}(x, w, \theta_{xw}) \end{aligned} \quad (34)$$

with

$$\begin{aligned} \theta_x &= (W_x^1, \dots, W_x^{x_D}, b_x^1, \dots, b_x^{x_D}); \\ \theta_{xw} &= (W_{xw}^1, \dots, W_{xw}^{xw_D}, b_{xw}^1, \dots, b_{xw}^{xw_D}) \\ \theta_w &= (W_w^1, \dots, W_w^{w_D}, b_w^1, \dots, b_w^{w_D}) \end{aligned} \quad (35)$$

and for a variable $v = x, w$ or mixed terms from (x, w) ,

$$\mathcal{D}_v(v, \theta_v) \equiv h_{v_D} \circ h_{v_{D-1}} \circ \dots \circ h_1(v) \quad (36)$$

and $h_i(v) = \sigma(W_v^i v + b_v^i)$ and $\sigma(\cdot)$ is an activation function, e.g. a RELU(v), ELU(v), tanh(v), or cRELU(v).

Example 1: Deep Koopman Learning on an 2 State System with a Single Input We first illustrate the use of deep control Koopman learning on a simple two state example system with a single input. Consider the system

$$\begin{aligned} x_{t+1}^1 &= -a_1 x_t^2 + a_3 x_t^1 \sin(\omega u_t) \\ x_{t+1}^2 &= \sin(\omega x_t^1) + a_2 x_t^2 + x_t^1 x_t^2 u_t \end{aligned} \quad (37)$$

where $a_1 = -0.96, a_2 = 0.88, a_3 = -0.95$, and $\omega = -2.0$. The input signal is defined as a step function

$$u_t = \begin{cases} 0 & t < 250 \\ 1 & t \geq 250. \end{cases} \quad (38)$$

A simulation of the system for the initial condition $x_0 = (0.5, -0.1)$ is given in Figure 1 and the outcome of a multi-step prediction task is given in Figure 1. 250 points of training data are provided to the Koopman learning algorithm, while the remaining 250 data points are withheld during training for test and evaluation. In Figure 1, we provide a single initial condition for which no forward prediction training data was provided and evaluate the predictive capability of the Koopman operator. We see in Figure 1 that the average error of the approximate input-Koopman operator learned by the deep neural networks is approximately 1%, per time-point, over a 120 step forward prediction task.

IV. MODEL DECOMPOSITION ALGORITHM

We now consider a system decomposition approach for nonlinear dynamical systems, where subsystems are selected to satisfy two criteria: 1) each subsystem's ability to infer its internal states given local output measurements is maximized, 2) the influence of all disturbances w_t from other subsystems on a given subsystem S_i is minimized.

We use the Koopman controllability and observability gramians to compute the decomposition criterion. Following the Koopman operator approach outlined in [12], we can

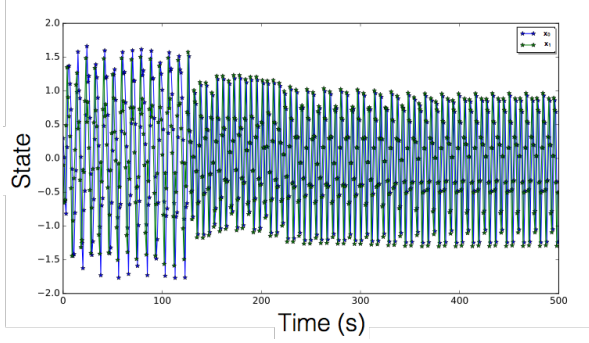


Fig. 1. The time-lapse response of a two-state control system to initial condition $x_0 = (0.5, -0.1)$ and a step input u_t . The output of the first state and second states, x_1^t and x_2^t are marked with blue and green dots respectively.

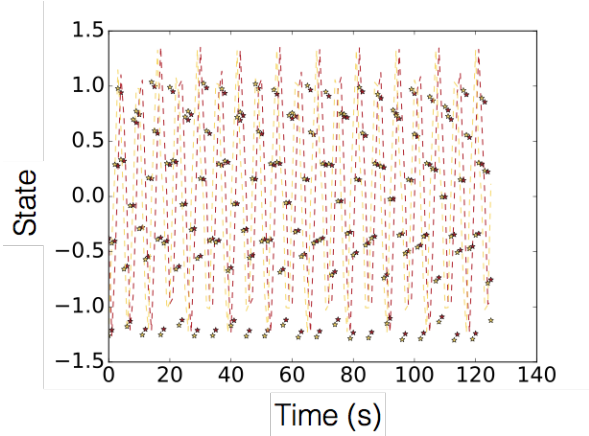


Fig. 2. Multi-step forward prediction (120 steps, plotted as dashed lines) for the system (plotted as dots) outlined in Example 1 .

define observability X_o^ψ and controllability gramian X_c^ψ

$$\begin{aligned} X_o^\psi &= \sum_{t=0}^{\infty} W_h^T (K_x^t)^T K_x^t W_h, \\ X_c^\psi &= \sum_{t=0}^{\infty} K_x^t K_u K_u^T (K_x^t)^T. \end{aligned} \quad (39)$$

As shown in [12], the Koopman gramians provide a direct approach for quantifying nonlinear controllability and nonlinear observability. When considering a linear time-invariant system, the Koopman gramians are identical to the original gramians. Furthermore, when a nonlinear system is locally controllable or observable, there exists a projection of the Koopman gramian that is positive definite.

In addition, the Koopman gramians characterize the input-output properties of the linear system defined by the control-Koopman operator. Thus, the traditional interpretations of output energy and input energy [24] can be articulated in terms of Koopman gramians. In particular, given an initial condition $\psi_x(x(0)) \in \mathbb{R}^{n_L}$, the energy of the output $y_t \in \mathbb{R}^p$ is given by

$$\|y_t\|_2^2 = y_t^T y_t = \psi_x(x_0)^T X_o^\psi \psi_x(x_0), \quad (40)$$

Moreover, given a target state x_0 , the minimum input energy is quantified using the inverse of the Koopman controllability gramian. As in classical linear systems theory, the inverse of the Koopman controllability gramian exists if the pair (K_x, K_u) is controllable.

$$\|\psi_w^{opt}\|_2^2 = \psi_x(x_0)^T (X_c^\psi)^{-1} \psi_x(x_0), \quad (41)$$

where $\|\psi_w^{opt}\|_2^2$ denotes the minimum disturbance energy to drive the system from $x_{-\infty} = 0$ to x_0 .

The Koopman gramians are n_L by n_L matrices. In particular, not every column in the Koopman gramian coincides with a physically meaningful state. However, leveraging Assumption 4, we have that the first n columns (or rows) of X_o^ψ and $(X_c^\psi)^{-1}$ are directly tied to the original state x contained within the observable function $\psi_x(x)$. Thus, instead of considering unit perturbations directly to the observable function $\psi(x)$ of the form

$$(\psi_x(x[0]) + e_i)^T X_o(\psi_x(x[0]) + e_i) \quad (42)$$

we consider unit perturbations along the first n observable functions, coinciding with *actual physical states* of the system.

$$\|\psi_x(x(t))^T \psi_x(x(t))\| = \psi_x(x[0] + e_i)^T X_i^\psi \psi_x(x[0] + e_i) \quad (43)$$

where $X_i^\psi = X_o^\psi$ or $X_i = (X_c^\psi)^{-1}$. The Koopman observability and controllability gramian are thus used to efficiently compute the energy of the input-output response, in response to unit perturbations to the input of the nonlinear function of $\psi_x(x)$.

Based on our decomposition criterion, for one subset S_i of original states x , we define

$$\begin{aligned} \kappa_{S_i}^o &= \frac{\psi_x(x = I_{S_i})^T X_o^\psi \psi_x(x = I_{S_i})}{\psi_x(x = (I - I_{S_i}))^T X_o^\psi \psi_x(x = (I - I_{S_i}))}, \\ \kappa_{S_i}^c &= \frac{\psi_x(x = I_{S_i})^T (X_c^\psi)^{-1} \psi_x(x = I_{S_i})}{\psi_x(x = (I - I_{S_i}))^T (X_c^\psi)^{-1} \psi_x(x = (I - I_{S_i}))}, \end{aligned} \quad (44)$$

where I is the n -dimension vector whose elements are all 1, I_{S_i} is the vector that states in S_i are 1 while the rest is 0. We can see that $\kappa_{S_i}^o$ expresses this subsystem's ability to infer its internal states compared to other subsystems given local output measurement. In the meanwhile, $\kappa_{S_i}^c$ reveals the influence of disturbances from other subsystems on subsystem S_i compared to its own internal disturbances. We want both to be maximized simultaneously. We define our objective function as a linearization of these two terms.

$$\kappa_{S_i} = \kappa_{S_i}^o + \lambda \kappa_{S_i}^c, \quad (46)$$

where λ is a positive constant to reveal the relative important of $\kappa_{S_i}^o$ and $\kappa_{S_i}^c$ in our concerns. Because usually $\kappa_{S_i}^o$ and $\kappa_{S_i}^c$ are with different magnitudes, we normalize the term by its average value before we do the decomposition. Also, in many applications, it is better to optimize the worst

case $\min_{S_1, \dots, S_k} (\kappa_{S_i})$, so we get the following optimization problem to decompose the system into k subsystems:

$$\begin{aligned} \max \quad & \min_{S_1, \dots, S_k} \kappa_{S_i} \\ \text{s.t.} \quad & \cup S_i = x, \quad \cap S_i = \emptyset, \quad \forall i \end{aligned} \quad (47)$$

However, there are two issues with this optimization. First, it is NP-hard that all possible set of subsystems is combinatorial number. Second, it is not a convex problem. We thus consider the following relaxations. First, suppose that S_i and κ_{S_i} both are continuous set; then we can verify (47) can be approximated by

$$\begin{aligned} \min \quad & \max_{S_1, \dots, S_k} \kappa_{S_i} \\ \text{s.t.} \quad & \cup S_i = x, \quad \cap S_i = \emptyset, \quad \forall i. \end{aligned} \quad (48)$$

Note that in ideal situation, (47) and (48) will result in an equal partition which means $\kappa_{S_i} = \kappa_{S_j}, \forall i, j$. So we can relax the original problem as follows

$$\begin{aligned} \min \quad & \sum_{i,j} |\kappa_{S_i} - \kappa_{S_j}| \\ \text{s.t.} \quad & \cup S_i = x, \quad \cap S_i = \emptyset, \quad \forall i \end{aligned} \quad (49)$$

Although the (49) is still NP-hard, it gives us more intuition about the nature of the problem. As we can see, the (49) is trying to minimize the total difference among subsystems. That is, we want the decomposition to result in a more balanced partition, where balance is defined in terms of subsystem controllability (κ_c) and subsystem observability (κ_o).

This problem is equivalent to the multi-way number partitioning problem. [25] gives an efficient and error-bounded heuristic algorithm to approximate the optimal solution. While [25] only considers minimizing the difference among sum of numbers in each subset, our problem is more complicated because when we introduce a new state into the cluster, the objective function can not be computed by directly adding the value of new state and the original rank value of the cluster, since this would require that the Koopman observable is linear in the state x_t . We thus propose a revised version of the original algorithm that accounts for the nonlinearity of the Koopman observable function (see Figure 3). Note that this algorithm does not consider the underlying connections in the network. For the application who has this requirement. We can slightly change the algorithm such as each time, we choose the neighborhood nodes of the clusters to do the update.

V. DECOMPOSITION OF AN IEEE-39 BUS SYSTEM

In this section we apply our Koopman controllability and observability decomposition algorithm on a swing dynamics model for the IEEE 39 bus system. We consider the problem of modeling disturbances to the swing dynamics; specifically, we model perturbations to the relative speed and relative angle states of individual generators. The perturbed system dynamics, assuming a disturbance Δ_i to the initial condition

K-way Partitioning function (a, k)

Input : Array a and cluster number k , each $a[j]$ is the value of κ_{S_i} when S_i only contains state j .

Output: k clusters and $\kappa_{S_i}^o$ and $\kappa_{S_i}^c$ for each cluster S_i . Initialize an empty heap $heap()$

for $a_j \in a$ **do**

- Construct tuple set: $b_i = \langle a_i, \underbrace{0, 0, \dots}_{k-1} \rangle$.
- Define b_i^{\max} as the first element in tuple b_i , also for each element in b_i , we will have a label to reveal if this element is a member of x_t or an auxiliary Koopman observable function (not a state variable).
- $heap.push(b_i)$.

end

while *More than one tuple remains* **do**

- $b_i^{\max} = heap.pop()$ ## largest element
- $b_j^{\max} = heap.pop()$ ## second largest element
- for** each permutation p for $[1, \dots, k]$ **do**

 - Define $b_{new} = b_i^{\max} \cup b_j^{\max}(p)$, \cup is element-wise operator, p means that b_j^{\max} rearranged by the permutation p .
 - Compute κ_{S_i} for each dimension of b_{new} and record b_{new}^{\max} and corresponding p
 - Record b^{out} as the minimum of b_{new}^{\max} and the corresponding p^{out} .

- end**
- $b^{in} = b_i^{\max} \cup b_j^{\max}(p^{out})$
- Compute κ_{S_i} for each dimension of b^{in} and put value into the corresponding dimension (insert in the first slot of the array).
- Normalize the first place's value of each dimension by their minimum.

end

cluster = $heap.pop()$, compute $\kappa_{S_i}^o$ and $\kappa_{S_i}^c$ for each cluster.

return [cluster, $\kappa_{S_i}^o, \kappa_{S_i}^c$]

Fig. 3. Koopman gramian multi-way partitioning algorithm

of the relative angle $\delta_i(0)$ is modeled as

$$\begin{aligned} \dot{\delta}_i &= \omega_i + \mathcal{D}(\Delta_i + \delta_i(0)) = \omega_i + 1u_i(t), \\ \dot{\omega}_i &= \frac{1}{M_i} (-D_i \omega_i + P_{m,i} - P_{e,i}) + \mathcal{D}(\Omega_i + \omega_i(0)), \end{aligned} \quad (50)$$

where conservation of power flow dictates

$$P_{e,i} = V_i \sum_{j=1}^n V_j (G_{ij} \cos(\delta_i - \delta_j) + B_{ij} \sin(\delta_i - \delta_j)). \quad (51)$$

where G_{ij} and B_{ij} are the transfer conductance and susceptance between buses i and j , and $i = 1, \dots, n$, where $n = 9$. Here we have taken generator 10 as a reference frame for the relative speed ω_i and relative angle δ_i of

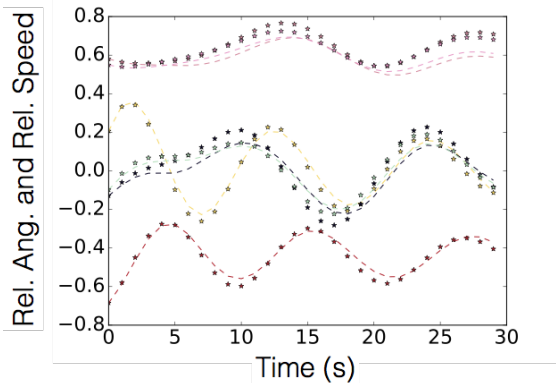


Fig. 4. A figure showing the multi-step time-lapse prediction (dashed lines) of a deep input-Koopman operator learned from training time-series data of the 39 bus system, using 100 random initial conditions for the relative speed and relative angle. The ground truth is plotted as dots.

each system. The nonlinearity of the power flow equations couple directly into the swing dynamics, defining an implicit nonlinear dynamical system with sinusoidal terms.

We consider a Koopman operator approach, motivated by several observations [26]. First, our approach is data-driven, which is suitable for wide-area monitoring applications when working with uncalibrated or parametrically varying models (due to changes in operational context or uncertainty). Second, the approach is potentially scalable, since an increase in the number of system states can be captured using larger Koopman dictionaries, generated by scalable deep learning algorithms in Tensorflow. Third, Koopman modes naturally reveal coherency or incoherency among generators [27], [26], which can be useful for distributed control design and transient stability analysis [14], [28].

We trained an input-Koopman operator for the 39 bus using our deep dynamic mode decomposition algorithm. We implemented a 20-wide, 10 layer deep ResNet with exponential linear unit activation functions (ELUs) [29] and Dropout [30] in TensorFlow. We generated 100 random trajectories of the IEEE 39 bus swing dynamics (1 second resolution) and used 50 of the trajectories as training data for learning a deep Koopman operator. The remaining 50 trajectories were reserved for the test stage. All trajectories were defined on a normalized scale, to ensure convergence of the Adam optimizer. Model accuracy was evaluated in two ways: 1) one-step prediction error on test data (less than 0.01%) and 2) multi-step prediction error on a previously unseen initial condition drawn from the test data (less than 0.4% error per time-step). The results of the multi-step prediction task are plotted in Figure 4.

We next applied our decomposition algorithm to compute a partition on the generators (see Figure 6) that accounted for balancing of κ_o (subsystem observability) and κ_c (subsystem controllability). This decomposition results in subsystems that maximize internal observability while simultaneously maximizing resiliency to external disturbances. The raw values of κ_o and κ_c for each generator are plotted in Figure 5. We noted that generator 2 exhibited high κ_o scores, but

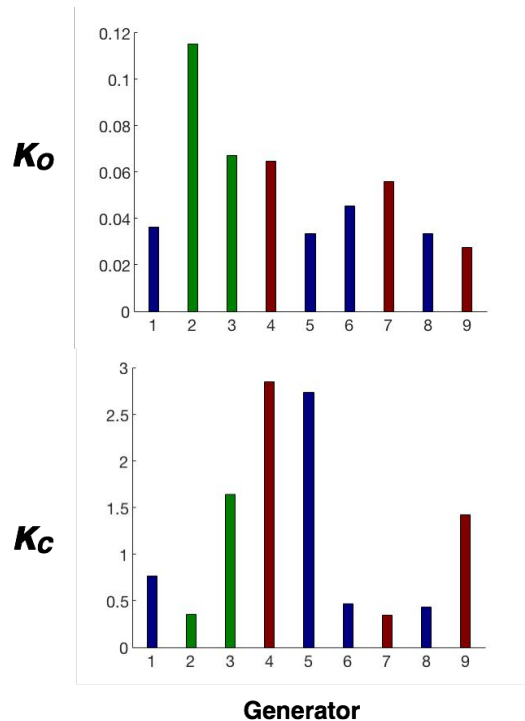


Fig. 5. Bar charts of κ_o (subsystem relative observability) and κ_c (subsystem relative controllability) for each generator.

had a low κ_c score, indicating susceptibility to external disturbances from other generators in the swing equations.

Our algorithm identified a clustering of generators resulting in a maximum variation in κ_c of

$$\max_{i,j} |\kappa_{c,i} - \kappa_{c,j}| = 0.33434$$

and a maximum variation in κ_o of

$$\max_{i,j} |\kappa_{o,i} - \kappa_{o,j}| = 0.09744.$$

Since our algorithm normalized the contributions of both κ_c and κ_o , we were able to balance despite the separation in scales. Interestingly, our algorithm identified zonal clusterings for generators that were for the most part closer to each other than generators outside their cluster (see Figure 6). However, this was not always the case; generator 6 exhibited a weak κ_c score and relatively weak κ_o score and thus was included in a separate clustering to ensure balanced subsystem controllability and observability across clusters. These observations illustrate the input-output focus of our Koopman decomposition approach. Whereas area assignments are often allocated based on spatial criteria, our algorithm seeks to minimize subsystem sensitivity to disturbances from other subsystems and internal observability, to ensure accurate state estimation [31].

VI. CONCLUSION

In this paper we introduced a method for learning input-Koopman operators from data by integrating deep learning and dynamic mode decomposition. In particular, we

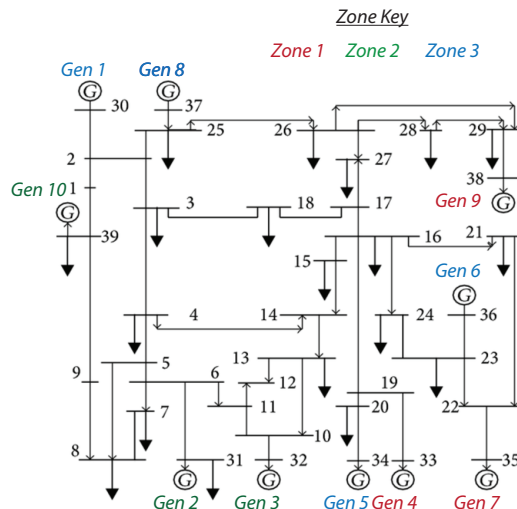


Fig. 6. A figure showing the area/zone assignment of generators by our modified multi-way partitioning algorithm, based on Koopman controllability and observability.

explored the conditions under which a input-state separable form exists for the input-Koopman equations, enabling construction of Koopman gramians. We showed that deep dynamic mode decomposition is able to recover a high fidelity approximation involving input-state separable Koopman operators, even when the underlying system is not input-state separable. These results underscore the power of learning representations for approximate data-driven control. We introduced a nonlinear decomposition algorithm, based on Koopman gramians, that maximizes internal subsystem observability and disturbance rejection from unwanted noise in other subsystems. Future work will focus on scalability and analysis of system with hybrid dynamics.

REFERENCES

- [1] Sergi Regot, Javier Macia, Núria Conde, Kentaro Furukawa, Jimmy Kjellén, Tom Peeters, Stefan Hohmann, Eulàlia de Nadal, Francesc Posas, and Ricard Solé. Distributed biological computation with multicellular engineered networks. *Nature*, 469(7329):207, 2011.
- [2] Melissa B Miller and Bonnie L Bassler. Quorum sensing in bacteria. *Annual Reviews in Microbiology*, 55(1):165–199, 2001.
- [3] Alvin Tamsir, Jeffrey J Tabor, and Christopher A Voigt. Robust multicellular computing using genetically encoded nor gates and chemical wires. *Nature*, 469(7329):212, 2011.
- [4] Nai-Yuan Chiang and Victor M Zavala. Large-scale optimal control of interconnected natural gas and electrical transmission systems. *Applied Energy*, 168:226–235, 2016.
- [5] Tao Li, Mircea Eremia, and Mohammad Shahidehpour. Interdependency of natural gas network and power system security. *IEEE Transactions on Power Systems*, 23(4):1817–1824, 2008.
- [6] Silvio J Pereira-Cardenal, Birger Mo, Anders Gjelsvik, Niels D Riegels, Karsten Arnbjerg-Nielsen, and Peter Bauer-Gottwein. Joint optimization of regional water-power systems. *Advances in Water Resources*, 92:200–207, 2016.
- [7] Silvio J Pereira-Cardenal, Henrik Madsen, Karsten Arnbjerg-Nielsen, Niels Riegels, Roar Jensen, Birger Mo, Ivar Wangensteen, and Peter Bauer-Gottwein. Assessing climate change impacts on the iberian power system using a coupled water-power model. *Climatic change*, 126(3-4):351–364, 2014.

- [8] Mung Chiang and Tao Zhang. Fog and iot: An overview of research opportunities. *IEEE Internet of Things Journal*, 3(6):854–864, 2016.
- [9] Mung Chiang, Steven H Low, A Robert Calderbank, and John C Doyle. Layering as optimization decomposition: A mathematical theory of network architectures. *Proceedings of the IEEE*, 95(1):255–312, 2007.
- [10] Rubén J Sánchez-García, Max Fennelly, Seán Norris, Nick Wright, Graham Niblo, Jacek Brodzki, and Janusz W Bialek. Hierarchical spectral clustering of power grids. *IEEE Transactions on Power Systems*, 29(5):2229–2237, 2014.
- [11] Fredrik Raak, Yoshihiko Susuki, Takashi Hikihara, Harold R Chamorro, and Mehrdad Ghandhari. Partitioning power grids via nonlinear koopman mode analysis. In *Innovative Smart Grid Technologies Conference (ISGT), 2014 IEEE PES*, pages 1–5. IEEE, 2014.
- [12] Enoch Yeung, Soumya Kundu, and Nathan Hodas. A koopman operator approach for computing and balancing gramians for discrete time nonlinear systems. *arXiv*, 2017.
- [13] Igor Mezić and Andrzej Banaszuk. Comparison of systems with complex behavior. *Physica D: Nonlinear Phenomena*, 197(1):101–133, 2004.
- [14] Igor Mezić. Spectral properties of dynamical systems, model reduction and decompositions. *Nonlinear Dynamics*, 41(1):309–325, 2005.
- [15] Clarence W Rowley, Igor Mezić, Shervin Bagheri, Philipp Schlatter, and Dan S Henningson. Spectral analysis of nonlinear flows. *Journal of fluid mechanics*, 641:115–127, 2009.
- [16] Matthew O Williams, Ioannis G Kevrekidis, and Clarence W Rowley. A data-driven approximation of the koopman operator: Extending dynamic mode decomposition. *Journal of Nonlinear Science*, 25(6):1307–1346, 2015.
- [17] Danial Trudnowski, Matt Donnelly, and Eric Lightner. Power-system frequency and stability control using decentralized intelligent loads. In *Proceedings of the 2005/2006 IEEE Power and Energy Society Transmission and Distribution Conference and Exposition*, pages 1453–1459, 2006.
- [18] Joshua L Proctor, Steven L Brunton, and J Nathan Kutz. Generalizing koopman theory to allow for inputs and control. *arXiv preprint arXiv:1602.07647*, 2016.
- [19] Joshua L Proctor, Steven L Brunton, and J Nathan Kutz. Dynamic mode decomposition with control. *SIAM Journal on Applied Dynamical Systems*, 15(1):142–161, 2016.
- [20] Bernard O Koopman. Hamiltonian systems and transformation in hilbert space. *Proceedings of the National Academy of Sciences*, 17(5):315–318, 1931.
- [21] BO Koopman and J v Neumann. Dynamical systems of continuous spectra. *Proceedings of the National Academy of Sciences*, 18(3):255–263, 1932.
- [22] Enoch Yeung, Soumya Kundu, and Nathan Hodas. Learning deep neural network representations for koopman operators of nonlinear dynamical systems. *arXiv preprint arXiv:1708.06850*, 2017.
- [23] Qianxiao Li, Felix Dietrich, Erik M Bollt, and Ioannis G Kevrekidis. Extended dynamic mode decomposition with dictionary learning: a data-driven adaptive spectral decomposition of the koopman operator. *arXiv preprint arXiv:1707.00225*, 2017.
- [24] Geir E Dullerud and Fernando Paganini. *A course in robust control theory: a convex approach*, volume 36. Springer Science & Business Media, 2013.
- [25] Richard E Korf. Multi-way number partitioning. In *IJCAI*, pages 538–543, 2009.
- [26] Yoshihiko Susuki, Igor Mezić, Fredrik Raak, and Takashi Hikihara. Applied koopman operator theory for power systems technology. *Nonlinear Theory and Its Applications, IEICE*, 7(4):430–459, 2016.
- [27] Yoshihiko Susuki and Igor Mezić. Nonlinear koopman modes and coherency identification of coupled swing dynamics. *IEEE Transactions on Power Systems*, 26(4):1894–1904, 2011.
- [28] Alexandre Mauroy and Igor Mezić. Global stability analysis using the eigenfunctions of the koopman operator. *IEEE Transactions on Automatic Control*, 61(11):3356–3369, 2016.
- [29] Djork-Arné Clevert, Thomas Unterthiner, and Sepp Hochreiter. Fast and accurate deep network learning by exponential linear units (elus). *arXiv preprint arXiv:1511.07289*, 2015.
- [30] Nitish Srivastava, Geoffrey E Hinton, Alex Krizhevsky, Ilya Sutskever, and Ruslan Salakhutdinov. Dropout: a simple way to prevent neural networks from overfitting. *Journal of machine learning research*, 15(1):1929–1958, 2014.

- [31] Milan Korda and Igor Mezić. Linear predictors for nonlinear dynamical systems: Koopman operator meets model predictive control. *arXiv preprint arXiv:1611.03537*, 2016.